Journal of Experimental Botany
doi:10.1093/jxb/erz482 Advance Access Publication 28 October 2019
This paper is available online free of all access charges (see https://academic.oup.com/jxb/pages/openaccess for further details)

RESEARCH PAPER

PAMP-INDUCED SECRETED PEPTIDE 3 modulates immunity in Arabidopsis

Javad Najafi[1], Tore Brembu[1], Ane Kjersti Vie[1], Rannveig Viste[1,*], Per Winge[1], Imre E. Somssich[2] and Atle M. Bones[1,†]

[1] Cell, Molecular Biology and Genomics Group, Department of Biology, Norwegian University of Science and Technology, 7491 Trondheim, Norway
[2] Department of Plant Microbe Interactions, Max Planck Institute for Plant Breeding Research, Carl-von-Linné-Weg 10, 50829 Cologne, Germany

* Present address: Department of Neurology, Laboratory of Clinical Neurophysiology, Oslo University Hospital, 0450 Oslo, Norway.
† Correspondence: atle.m.bones@ntnu.no

Received 13 February 2019; Editorial decision 17 October 2019; Accepted 18 October 2019

Editor: Steven Spoel, University of Edinburgh, UK

Abstract

Small post-translationally modified peptides are important signalling components of plant defence responses against phytopathogens, acting as both positive and negative modulators. PAMP-INDUCED SECRETED PEPTIDE (PIP) 1 and 2 have been shown to amplify plant immunity. Here we investigate the role of the related peptide PIP3 in the regulation of immune response in Arabidopsis. Treatment with synthetic PIP peptides led to similar transcriptome reprogramming, indicating an effect on innate immunity-related processes and phytohormones, including jasmonic acid (JA) biosynthesis and signalling. *PIP3* overexpressing (OX) plants showed enhanced growth inhibition in response to flg22 exposure. In addition, flg22-induced production of reactive oxygen species and callose deposition was significantly reduced in *PIP3-OX* plants. Interestingly, *PIP3-OX* plants showed increased susceptibility toward both *Botrytis cinerea* and the biotrophic pathogen *Pseudomonas syringae*. Expression of both JA and salicylic acid (SA) biosynthesis and signalling genes was more induced during *B. cinerea* infection in *PIP3-OX* plants compared with wild-type plants. Promoter and ChIP-seq analyses indicated that the transcription factors WRKY18, WRKY33, and WRKY40 cooperatively act as repressors for *PIP3*. The results point to a fine-tuning role for PIP3 in modulation of immunity through the regulation of SA and JA biosynthesis and signalling pathways in Arabidopsis.

Keywords: Arabidopsis, biotic stress, *Botrytis cinerea*, PAMP-induced secreted peptide, peptide ligand, transcriptome.

Introduction

As sessile organisms, plants have developed sophisticated communication systems between cells and tissues, especially when dealing with a constantly challenging environment. They are continuously attacked by diverse phytopathogens including viruses, bacteria, fungi, and nematodes. Resistance or susceptibility is determined by successful strategies employed by the plant or the invading microbe. Pathogen-associated molecular pattern (PAMP)-triggered immunity (PTI) acts as the first active response to microbial perception and is thought to be an ancient form of immunity (Chisholm *et al.*, 2006; Jones and Dangl, 2006). PTI is activated upon perception and recognition of PAMPs by specific pattern-recognition receptors (PRRs) on the cell membrane. PRR activation is followed by a burst of Ca^{2+} and reactive oxygen species (ROS), activation of mitogen-activated protein (MAP) kinase signalling cascades, transcriptional reprogramming, deposition of callose at the site

of infection to reinforce the cell wall against pathogen penetration, and stomatal closure (Ligterink *et al.*, 1997; Gómez-Gómez and Boller, 2000; Nürnberger *et al.*, 2004; Melotto *et al.*, 2006; Luna *et al.*, 2011). Plant responses to pathogens are also associated with the transcriptional reprogramming of a large number of host genes after pathogen attack, including genes encoding transcription factors (TFs) involved in regulation of plant defence responses. The WRKY family of TFs have been comprehensively investigated with regard to plant defence responses. WRKY18, WRKY40, and WRKY33 have been shown to actively regulate the expression of numerous genes in response to pathogens and flg22 treatment. WRKY33 has been found to have an enhanced activation in the salicylic acid (SA)-related host response as well as reduced activation in the jasmonic acid (JA)-associated responses when infected with *B. cinerea*. (Qiu *et al.*, 2008; Pandey *et al.*, 2010; Birkenbihl et al., 2012, 2017; Liu *et al.*, 2015).

ROS generation is one of the very early responses to biotic and abiotic stimuli including PAMPs (Felix *et al.*, 1999; Baxter *et al.*, 2014). The ROS produced auotopropagates as a wave, travelling rapidly through the apoplast of neighbouring cells and activating a systemic response to the stimuli (Karpinski *et al.*, 1999; Miller *et al.*, 2009). In order to act as a signalling molecule, a non-toxic level of ROS between production and scavenging should be maintained (Mittler *et al.*, 2004). Signalling pathways initiated by ROS have many intersections with other signalling components, including calcium, mitogen-activated protein kinases, phytohormones, and TFs, and play a vital role in fine-tuning of plant responses to developmental programmes and stress conditions (Gilroy *et al.*, 2014; Xia *et al.*, 2015; Sewelam *et al.*, 2016).

Immune responses can also be induced by endogenous molecules produced upon pathogen attack. Among several classes of endogenous elicitors, active peptides have attracted attention for their role in regulation of plant immunity (Boller and Flury, 2012). AtPEP1 was the first peptide with damage-associated molecular pattern (DAMP) activity purified from Arabidopsis (Huffaker *et al.*, 2006). The Arabidopsis genome encodes eight peptides with similar structure to PROPEP1 that are perceived by two receptor-like kinases, PEP-RECEPTOR 1 (PEPR1) and PEP-RECEPTOR 2 (PEPR2) (Krol *et al.*, 2010; Yamaguchi *et al.*, 2010). Another example is phytosulfokine (PSK), originally identified as a regulator of plant growth and development (Matsubayashi and Sakagami, 1996; Hanai *et al.*, 2000). PSKs can also regulate plant immunity against biotrophic and necrotrophic pathogens in an antagonistic manner through their receptor PSKR1 and are proposed to act as part of a fine-tuning system in growth–defence trade-offs (Igarashi *et al.*, 2012; Mosher *et al.*, 2013).

Recently, two members of a new peptide family termed PAMP-INDUCED SECRETED PEPTIDES (PIPs), PIP1 and PIP2, were shown to amplify immunity through RECEPTOR-LIKE KINASE 7 (RLK7) in Arabidopsis (Hou *et al.*, 2014). Plants overexpressing *prePIP1* and *prePIP2* showed increased resistance against *Pseudomonas syringae* and *Fusarium oxysporum*. The PIP family consists of eleven members (PIP1 to 3 and PIP-LIKE (PIPL) 1 to 8); several of the family members are transcriptionally induced by biotic and/or abiotic stress (Hou *et al.*, 2014; Vie *et al.*, 2015). PIP and PIPL propeptides are short (<115 amino acids), with N-terminal aliphatic residues predicted as signal peptide and a C-terminal conserved motif (SGPS) believed to act as a part of biologically active peptides. PIP2 and PIP3 possess two SGPS motifs at the C-termini of the encoded prepropeptides (Hou *et al.*, 2014; Vie *et al.*, 2015).

Here, we present a functional study of PIP3 (At2g23270), another member of this family with high sequence similarity to PIP2. Ectopic application of the conserved C-terminal region of PIP1, PIP2, and PIP3 followed by gene expression analysis by microarray and real-time quantitative reverse transcription–PCR (qRT-PCR) revealed that many marker genes involved in immunity responses were differentially regulated by this treatment. *PIP3* loss-of-function plants challenged by *P. syringae* and *Botrytis cinerea* did not exhibit an altered phenotype, but plants overexpressing *prePIP3* were susceptible to both pathogens compared with wild-type (WT) plants. Production of ROS and callose deposition in response to flg22 were also impaired in *PIP3:OX* plants. Gene expression analysis of *B. cinerea*-infected plants showed that key genes involved in JA and SA biosynthesis and signalling pathways were up-regulated in overexpressing plants. These findings suggest that signalling initiated by PIP3 is involved in fine-tuning of plant immune responses to pathogens with different lifestyles.

Materials and methods

Plant material

All experiments were conducted with Arabidopsis Columbia-0 (Col-0) WT and mutants selected in Col-0 background. A dSpm transposon insertion mutant from the JIC_SM collection (Tissier *et al.*, 1999), *pip3* (SM_3_22412), *fls2* (SALK_026801), *rlk7* (SALK_094492H), and a T-DNA insertion mutant, *pip2-1* (SAIL_1275_B11; Sessions *et al.*, 2002), were obtained from Nottingham Arabidopsis Stock Centre. *wrky18*, *wrky40*, and *wrky18/40* lines were described by Pandey *et al.* (2010) and *wrky33* plants were described by Birkenbihl *et al.* (2012). Homozygous plants were screened based on growth on selectable medium and PCR using a combination of gene-specific and transposon or T-DNA-specific primers (Supplementary Table S1 at *JXB* online). Due to the very low expression of *PIP* genes under normal conditions, we induced their expression with flg22 treatment (see below), and null functionality was confirmed at the mRNA level. Overexpression lines of *PIP3* (At2g23270) were generated by PCR amplification of coding sequences from Col-0 plants and subsequent cloning into the destination vector pEG100 (Earley *et al.*, 2006) under control of the 35S promoter using Gateway technology. The construct was introduced to *Agrobacterium tumefaciens* strain C58C1 pGV2260 and transformed into Col-0 WT plants using the floral dip method (Clough and Bent, 1998). Independent transgenic T3 lines with a single copy of T-DNA and constitutive expression of *PIP3* were screened for further analysis.

Peptide treatments

Col-0 seeds were surface sterilized and sown on half-strength Murashige and Skoog (MS) agar plates (0.6% w/v) supplemented with 2% sucrose at a density of 15 seeds per Petri dish. Seeds were stratified at 4 °C for 2 d and transferred to growth room under 16 h (70 μmol m^{-2} s^{-1})–8 h light–dark photoperiod at 22 °C for 2 weeks. Seedlings were treated by spraying with an aqueous peptide solution (100 nM) supplemented with 0.02% (w/v) Silwet L-77 (Lehle Seeds, Round Rock, TX, USA). The peptide sequences were selected from the C-terminus of PIP propeptides consisting of the conserved SGPS motif as follows: PIP1:

EKMKSTVDSW[10]FQRLASGPSP[20]RGRGH; PIP2: SLGSIKDSGP[10] SPGEGHKVVD[20]RKDTFRFVKH[30]SGPSPSGPGH[40]; PIP3: SLGAI KESGP[10]SSGGEGHRFV[20]DRTETLEYGK[30]HSGPSTSGPG[40]H; and mock peptide: LSPGKNLSAP[10]GRVGSNPFTK[20]LRGS, which is derived from a randomized consensus sequence of IDL/PIP peptides (Vie *et al.*, 2015). Peptides were synthesized with a purity of >95% by Biomatik (Cambridge, Ontario, Canada). Control treatment was performed using MQ water and Silwet L-77. Vacuum infiltration was applied in a vacuum chamber at 20 inches Hg (50.8 cmHg) for 1 min to ensure that peptides penetrated into the tissue. Three hours after treatment, rosette leaves were harvested in three biological replicates. Each replicate consisted of material pooled from three Petri dishes.

Expression analyses

RNA isolation, cDNA synthesis and qRT-PCR, microarray experiments, statistical analysis, and Gene Ontology (GO) analysis were performed as described in Vie *et al.* (2015). Sequences of primers used in this study are listed in Supplementary Table S1. Genome-wide expression analysis was performed using the Arabidopsis (V4) Gene Expression Microarray 4×44K (Agilent Technology). The study is minimum information about a microarray experiment (MIAME) compliant. Raw data have been deposited in GEO, NCBI (accession number GSE79025). Gene ontology analysis and enrichment were performed after network integration and predicted gene functions using the GeneMANIA server (Mostafavi *et al.*, 2008).

Genome-wide chromatin immunoprecipitation sequencing (ChIP-seq) experiments were described and performed by Birkenbihl *et al.* (2012, 2017). The same datasets were used to retrieve WRKY33 and WRKY18/40 binding to *PIP1-3* promoter regions after *B. cinerea* and flg22 treatments, respectively.

Expression analysis, growth inhibitory, ROS production and callose deposition assays in response to flg22

For temporal expression analysis of *PIP* genes in response to flg22, seeds were grown for 2 weeks as described above for peptide treatment. Seedlings were sprayed with 100 nM flg22 and 0.02% (w/v) Silwet L-77, and MQ water and 0.02% (w/v) Silwet L-77 as control. Leaf tissue was harvested 1 min, 5 min, 10 min, 15 min, 30 min, 1 h, 6 h, and 24 h after treatment. For each time point, three biological replicates pooled from three Petri dishes each for treatment and control were harvested for RNA extraction. Growth inhibition assays were conducted as described by Igarashi *et al.* (2012). Seeds were germinated as described for peptide treatments. Four days after germination, seedlings were transferred to fresh liquid ½MS medium supplied with 2% sucrose and 100 nM flg22 in 24-well culture plates (one seedling in each well containing 1 ml of medium). The effect of flg22 treatment on seedling growth was measured after 10 d by measuring the fresh biomass of the seedlings. The whole experiment was repeated three times with similar result. Luminol-based ROS generation detection was performed as described by Bisceglia *et al.* (2015). Callose deposition assay was conducted as described by Luna *et al.* (2011) with some modifications. Seedlings were grown in six-well culture plates containing ½MS liquid culture supplemented by 2% sucrose for 6 d. At day 7, medium was replaced by either new ½MS as control or ½MS containing 1 μM flg22 as treatment. Twenty-four hours after treatment, seedlings were incubated in a mixture of ethanol: acetic acid (3:1 v/v) overnight or until all tissue became transparent. Samples were rehydrated in 70 mM phosphate buffer (pH 9.0) and stained in 0.01% (w/v) aniline blue in phosphate buffer for 2 h. Callose deposition in cotyledons was visualized with an epifluorescence microscope (NIKON Eclipse E800) using a UV filter, and callose deposition was quantified in ImageJ (Abràmoff *et al.*, 2004).

Pathogen assays

Pseudomonas syringae assays were performed as described by Lee *et al.* (2011). Seeds of different genotypes were grown in 2 ml of liquid ½MS supplemented by 2% sucrose in six-well culture plates (12 seedlings per well) for 6 d. At day 7, seedlings were transferred to new medium without sucrose and co-cultivated with *P. syringae* pv. *tomato* DC3000 at OD_{600}=0.02. Co-cultivated seedlings were washed with 70% ethanol and rinsed twice (for 10 s) to remove surface-attached bacteria. Three seedlings per replicate were placed into each of three 1.5 ml tubes containing 100 μl of water and ground with a pestle. Susceptibility was assessed in serial diluted samples as colony forming units (CFU) in WT, *fls2*, *pip3*, and *PIP3:OX* lines at 1, 2 and 3 d post-infection (dpi). A *P. syringae* assay was also conducted on 5-week-old plants grown in short day (10 h light–14 h dark) conditions. Leaf disks from fully grown leaves were used for susceptibility assessment as CFU described above.

A fungal pathogen assay was conducted as described by Birkenbihl *et al.* (2012). Briefly, plants were grown for 5 weeks under short day conditions (8 h light–16 h dark) in a growth chamber set to 20 °C and 80% humidity. Spores of *B. cinerea* isolate 2100 (CECT2; Spanish type) were diluted in Vogel buffer (43.86 mM sucrose, 11.63 mM Na-citrate, 28.7 mM K_2HPO_4, 0.81mM $MgSO_4.7H_2O$, 0.9 mM $CaCl_2{\cdot}2H_2O$, 24.98 mM NH_4NO_3) to a density of 2.5×10^5 spores ml^{-1}. For droplet inoculation and phenotype assay, 2 μl was applied to each side of fully developed leaves from 5-week-old plants. For mock treatment, only Vogel buffer was applied. For gene expression analysis higher concentrations of spores (5×10^5 spores ml^{-1}) were sprayed on plants, and leaf tissue was harvested for RNA isolation at 6, 12, and 24 h post-infection (hpi). Mock treatment was done only for 6 h, and changes of gene expression were measured relative to mock-treated plants at this time point. *In planta* pathogen growth assays were performed as described by Gachon and Saindrenan (2004). Briefly, droplet-infected leaves of plants were harvested 3 d after inoculation for DNA isolation. The relative ratio of *B. cinerea* and Arabidopsis DNA was determined by qPCR using pathogen (*Bc*CutA) and plant specific (*At*SKII) primers listed in Supplementary Table S1.

Results

Synthetic PIP1 and PIP2 C-terminal peptides alters the expression of stress responsive genes

PAMP-INDUCED SECRETED PEPTIDE 1 (*PIP1*) (At4g28460), *PIP2* (At4g37290), and *PIP3* (At2g23270) belong to a recently identified gene family with 13 members in the Arabidopsis genome, encoding peptides with similarity to INFLORESCENCE DEFICIENT IN ABSCISSION (IDA) and IDA-LIKE (IDL) peptides (Hou *et al.*, 2014; Vie *et al.*, 2015). An *in silico* co-expression analysis (ATTED-II; atted.jp, Obayashi *et al.*, 2018) showed that *PIP1*, *PIP2*, and *PIP3* are highly co-regulated under different experimental conditions (Supplementary Fig. S1A). The top 100 co-expressed genes for *PIP1*, *PIP2*, and *PIP3* were downloaded from ATTED-II, and a Venn diagram was made to represent the common sets of co-expressed genes (Supplementary Dataset S1). Our analysis revealed a high degree of overlap between the three gene lists, with 40 genes represented in the intersection category, further supporting a potential functional redundancy (Supplementary Fig. S1B). By comparison, only 18 genes were co-expressed with *PROPEP1*, *PROPEP2*, and *PROPEP3* (Supplementary Fig. S1C).

To improve our understanding of the downstream signalling pathways affected by these peptides, we designed synthetic peptides containing the C-terminal conserved domain of PIP1 (last 25 amino acids) and PIP2 (last 39 amino acids, including both conserved SGPS motives). Two-week-old WT plants were treated with 100 nM synthetic peptides for 3 h, and tissue was harvested for global transcriptome analysis. One hundred and ten genes (89 genes up-regulated, 21 genes down-regulated)

were significantly regulated (2-fold or more compared with control treatment, $P \leq 0.05$) by PIP1 peptide treatment. The transcriptome response to PIP2 treatment was stronger; 513 genes were differentially expressed (326 up-regulated and 187 down-regulated) using the same cut-off (Supplementary Dataset S2). Sixty-eight genes were similarly regulated by both peptides (Fig. 1A). Gene Ontology enrichment of regulated genes revealed that both peptide treatments affect biological pathways involved in plant responses to biotic and abiotic stresses and redox homeostasis (Fig. 1B, C). JA signalling genes, including *JAZ7*, *JAZ8*, and *JAZ9*, were among the most up-regulated genes by ectopic application of both peptides. Furthermore, other components of JA biosynthesis and signalling were differentially regulated in response to at least one of the peptides (Table 1). In contrast to the JA signalling pathway, few genes related to SA signalling were regulated. In addition, a number of ethylene-responsive TFs were also differentially regulated, including *ORA59*, *CEJ1*, and *GLIP1*, which play an important role in the integration of JA/ethylene (ET) and SA signalling cross-talk (Nakano *et al.*, 2006; Kwon *et al.*, 2009; Van der Does *et al.*, 2013; Table 1). The expression of nine genes involved in redox homeostasis, including *RRTF1*, *GRX480*, *GRXS13*, *GRXC11*, and *NTRB*, was also up-regulated by PIP2 peptide treatment.

Of 21 genes down-regulated by PIP1 treatment, 19 were also repressed by PIP2. Among these were genes involved in plant immune regulation, including *GLK1*, *CRK5*, *CRK15*, *CRK22*, and *WRKY60* TFs. More *CRKs* as well as other receptor-like kinases, especially LRR-RLKs, were also down-regulated only by PIP2 treatment (Supplementary Dataset S1). Based on functional categorization of up- and down-regulated genes, we speculated that PIP1 and PIP2, together with PIP3, might have a role in regulation of plant immunity. To evaluate the effect of PIP3, we repeated the experiment using PIP1, PIP2, and PIP3 C-terminal conserved domain peptides for analysis of innate immunity-related genes in response to these peptides. qRT-PCR analyses confirmed the differential regulation observed in the microarray experiments (Fig. 2A).

It has been reported that PIP1 amplifies plant immune response through RLK7 (Hou *et al.*, 2014). To test whether RLK7 also is involved in PIP3 perception, we analysed expression regulation of selected genes in *rlk7* and WT backgrounds in response to exogenous application of the synthetic PIP3 peptide. The majority of the selected genes responded similarly to PIP3 treatment in both WT and *rlk7* backgrounds (Fig. 2B). In the case of *JAZ9*, *RRTF1*, and *TAT3*, differential regulations were observed. *TAT3* regulation was found independent from PIP3 peptide treatment and similar deviations were also observed in control *rlk7* plants without treatment. These observations suggest that RLK7 is not a major receptor for PIP3.

PIP *genes are induced by flg22 and pathogen treatment*

The bacterial-derived PAMP flg22 is known as a strong inducer of PTI-related genes in Arabidopsis (Felix *et al.*, 1999). Previous transcriptome studies of flg22 responses in Arabidopsis indicate that *PIPs* are induced by endogenous and exogenous elicitors in WT plants but repressed in *fls2* mutants lacking the flg22 receptor (Denoux *et al.*, 2008; Lyons *et al.*, 2013; Supplementary Table S2). To get a better understanding of the dynamics of the response, a time course experiment on Arabidopsis seedlings treated by flg22 (100 nM) was performed. qRT-PCR analysis showed that the expression of all three genes started to increase significantly 15 min after treatment and reached a maximum at 30 min (Fig. 3A). *PIP1*, *PIP2*, and *PIP3* expression was induced 244-, 28- and 88-fold, respectively, at this time point. The expression levels of the analysed genes were still high after 1 h, but dropped to basal levels at later time points. flg22-induced expression of *PIPs* was completely abolished in *fls2* background (Fig. 3B).

The expression patterns of *PIP* genes in response to *B. cinerea* infection at 6, 12 and 24 h post-infection (hpi) were also studied. As shown in Fig. 3C, *PIP1* expression increased throughout the experiment, whereas *PIP2* and *PIP3* expression reached maximum levels at 12 hpi and declined at 24 hpi, with stronger induction observed for *PIP3*.

Identification of mutant and overexpression lines

To assign a biological function to the PIP peptides, we characterized putative knockout lines for *PIP2* (SAIL_1275_B11; *pip2*) and *PIP3* (SM_3_22412; *pip3*). The T-DNA insertion in *pip2* was placed 80 bp upstream of the start codon, whereas the En/Spm transposon insertion in *pip3* resulted in loss of the eight C-terminal amino acids, including a part of the last SGPS motif (Fig. 4A). Loss of *PIP3* expression in the *pip3* knockout line was confirmed (Fig. 4B). However, the *pip2* line showed increased *PIP2* expression both under normal growth conditions and after flg22 treatment (Fig. 4B). No T-DNA or transposon insertion lines for *PIP1* were found in available seed stocks. Due to the lack of proper null mutant lines for *PIP1* and *PIP2*, we focused on functional characterization of *PIP3*. Transgenic plants expressing *PIP3* coding sequence under control of the constitutive CaMV35S promoter were generated. Two independent T3 lines with constitutive expression of *PIP3* were chosen for further analysis. Under normal growth conditions, no significant growth or developmental abnormalities were observed in any of the lines (Supplementary Fig. S2).

PIP3 *overexpression alters responses to flg22 and pathogens*

flg22 is known to impede Arabidopsis seedling growth (Gómez-Gómez and Boller, 2000). We therefore examined the phenotype of the *pip3* mutant and constitutive *PIP3* overexpression lines by measuring the fresh weight (FW) of seedlings grown in the presence or absence of flg22. As shown in Fig. 5A, there were no significant differences between the examined lines grown in medium without flg22. In contrast, flg22 caused significant growth inhibition of *PIP3:OX* seedlings compared with WT seedlings, with an average FW reduction of 69% (*PIP3:OX6*) and 77% (*PIP3:OX7*) (Fig. 5A). Growth inhibition of *pip3* (53%) was comparable to WT (55%).

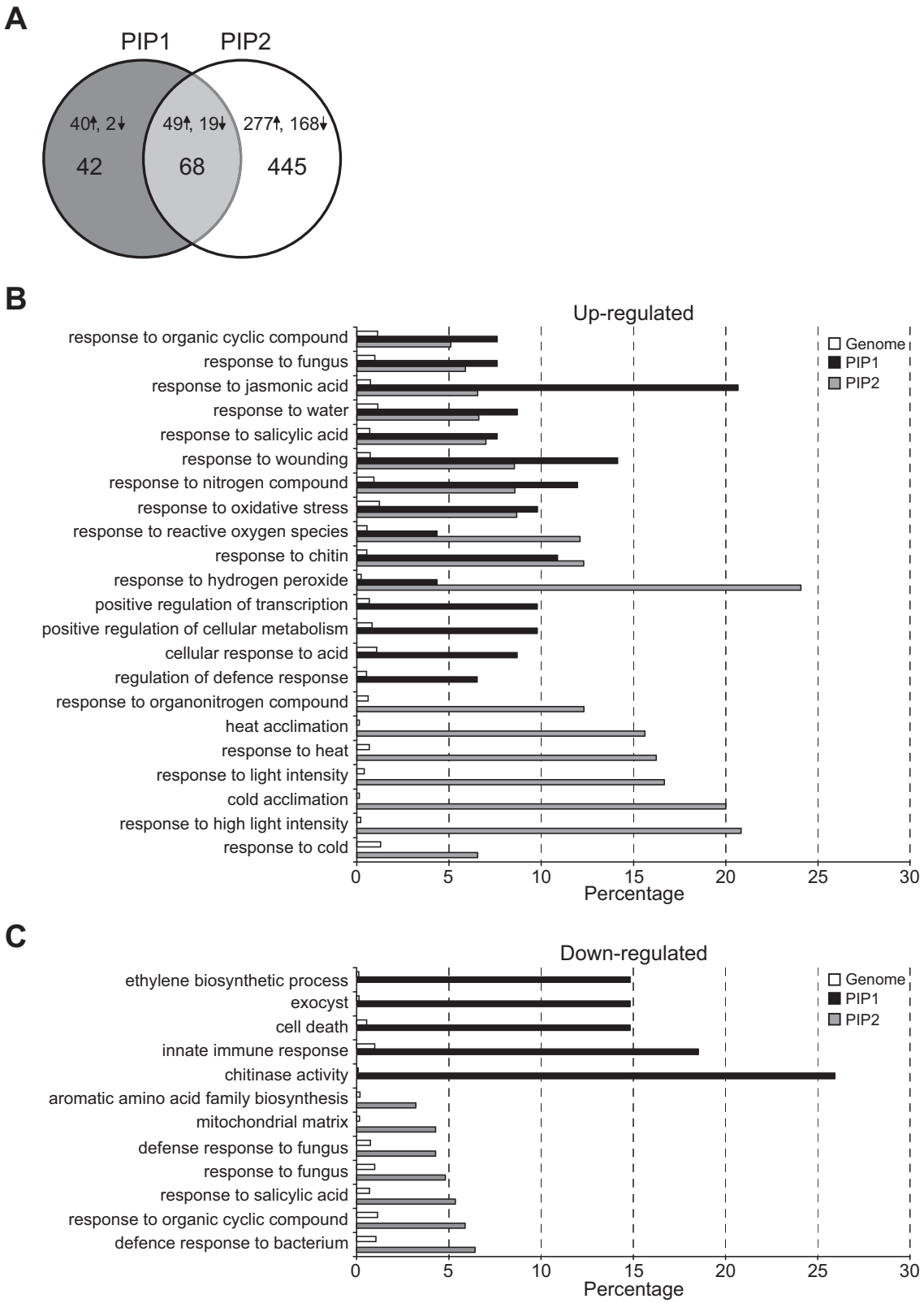

Fig. 1. Exogenous application of synthetic PIP1 and PIP2 C-terminal peptides cause transcriptome reprogramming. (A) Venn diagram representing number of genes significantly (P<0.05) regulated by PIP1 and PIP2 peptide treatment (100 nM, 3 h). Control seedlings were treated with water. (B, C) GO enrichment analysis of genes significantly up-regulated (B) and down-regulated (C) by PIP1 and PIP2 peptide treatment. The top 10 terms enriched terms in the gene set are listed. Bars show the frequency of each GO term in the PIP1/PIP2-responsive gene set and the genome.

Perception of flg22 is accompanied by a rapid and transient oxidative burst and ROS production followed by callose deposition that is diminished in *fls2* background (Felix *et al.*, 1999; Gómez-Gómez and Boller, 2000; Luna *et al.*, 2011). We used a luminol-based assay to evaluate ROS production in response to flg22 and PIP3 synthetic peptides in WT, *pip3* and

Table 1. Differentially regulated genes after PIP1 or PIP2 peptide treatment

Locus	Description	PIP1		PIP2	
		Fold change	Adjusted *P*-value	Fold change	Adjusted *P*-value
Jasmonic acid					
At2g34600	JAZ7 (jasmonate ZIM domain-containing protein 7)	7.78	0.0432	3.63	0.0329
At1g30135	JAZ8 (jasmonate ZIM domain-containing protein 8)	3.94	0.0241	2.20	0.0163
At1g70700	JAZ9 (jasmonate ZIM domain-containing protein 9)	3.25	0.0198	2.64	0.0086
At5g13220	JAZ10 (jasmonate ZIM domain-containing protein 10)	3.84	0.0198	1.79	0.0236
At1g17380	JAZ5 (jasmonate ZIM domain-containing protein 5)	2.87	0.0359	1.88	0.0238
At3g22275	JAZ13 (jasmonate ZIM domain-containing protein 13)	2.85	0.0284	NS	—
At1g74950	JAZ2 (jasmonate ZIM domain-containing protein 2)	1.92	0.0385	NS	—
At3g25760	AOC1 (allene oxide cyclase 1)	1.75	0.0475	1.91	0.0116
At1g17420	LOX3 (lipoxygenase 3)	1.70	0.0432	2.25	0.0243
At2g06050	OPR3 (OPDA-reductase 3)	1.83	0.0437	NS	—
At1g76680	OPR1 (OPDA-reductase 1)	NS	—	2.04	0.0254
At1g18020	OPR5 (OPDA-reductase 5)	NS	—	2.14	0.0254
At1g43160	RAP2.6 (RELATED TO APETALA2 6)	3.27	0.0290	3.34	0.0089
At1g32640	JIN1/MYC2 (JASMONATE INSENSITIVE 1)	2.62	0.0189	1.80	0.0099
At3g15500	ANAC055 (NAC domain-containing protein 55)	2.57	0.0176	3.46	0.0086
At1g52890	ANAC019 (NAC domain-containing protein 19)	2.55	0.0471	NS	—
At1g06160	ORA59 (octadecanoid-respoNSive AP2/ERF 59)	2.28	0.0297	NS	—
At3g48520	CYP94B3 (jasmonoyl-isoleucine-12-hydroxylase)	3.94	0.0437	3.58	0.0149
Salicylic acid					
At1g09415	NIMIN3 (NIM1-interacting 3)	NS	—	1.75	0.0389
At5g45110	NPR3 (NPR1-like protein 3)	NS	—	1.66	0.0422
At4g39030	SID1 (SALICYLIC ACID INDUCTION DEFICIENT 1)	NS	—	–1.56	0.017
At1g73805	SARD1 (SAR DEFICIENT 1)	–1.57	0.0432	–1.59	0.0126
At1g19250	FMO1 (flavin-dependent monooxygenase 1)	NS	—	–2.55	0.0291
At5g13320	PBS3 (avrPphB susceptible 3)	–1.81	0.0479	–2.74	0.0086
Redox homeostasis					
At4g34410	ERF109/RRTF1 (redox responsive transcription factor 1)	6.87	0.0176	7.26	0.0069
At1g28480	GRXC9 (glutaredoxin-C9)	NS		2.79	0.0187
At3g62950	GRXC11(glutaredoxin-C11)	NS		2.28	0.0120
At1g03850	GRXS13 (monothiol glutaredoxin-S13)	NS		2.15	0.0197
At2g29450	ATGSTU5 (glutathione *S*-transferase U5)	2.13	0.0479	3.01	0.0089
At1g10360	ATGSTU18 (glutathione *S*-transferase U18)	NS	—	2.02	0.0176
At2g29420	ATGSTU7 (glutathione *S*-transferase U5)	NS	—	1.76	0.0171
At2g25080	ATGPX1 (phospholipid hydroperoxide glutathione peroxidase 1)	NS	—	1.77	0.0431
At4g35460	NTRB (NADPH-dependent thioredoxin reductase B)	NS	—	1.66	0.0353
Immunity-related					
At5g46260	TIR-NBS-LRR class disease resistance protein	NS	—	3.10	0.0089
At4g19520	TIR-NBS-LRR class disease resistance protein	NS	—	2.87	0.0086
At5g46490	TIR-NBS-LRR class disease resistance protein	NS	—	2.26	0.0086
At1g63860	TIR-NBS-LRR class disease resistance protein	NS	—	2.21	0.0086
At1g76650	CML38 (calmodulin-like protein 38)	NS	—	3.41	0.0190
At4g20780	CML42 (calmodulin-like protein 42)	NS	—	2.64	0.0264
At3g44860	FAMT (farnesoic acid carboxyl-*O*-methyltransferase)	2.50	—	NS	0.0437
At2g30020	AP2C1 (protein phosphatase AP2C1)	1.65	—	2.35	—
At4g01250	WRKY22	NS	—	2.73	0.0086
At5g64810	WRKY51	NS	—	–1.99	0.0220
At4g23810	WRKY53	NS	—	–2.45	0.0122
At2g25000	WRKY60	–2.69	0.0437	–4.25	0.0086
At1g01720	ATAF1 (NAC transcription factor)	1.88	0.0413	2.04	0.0147
At1g21100	IGMT1 (indole glucosinolate *O*-methyltransferase 1)	2.11	0.0465	2.39	0.0113
At3g14210	ESM1 (EPITHIOSPECIFIER MODIFIER 1)	NS	—	–2.79	0.0440
At2g39200	MLO12 (MLO-like protein 12)	–2.18	—	–1.58	—
At3g45290	MLO3 (MLO-like protein 3)	NS	—	–1.48	—
At2g20570	GLK1 (Golden2-like protein 1)	–2.39	—	–3.16	—
At5g44190	GLK2 (Golden2-like protein 2)	NS	—	–2.68	—
At2g24850	TAT3 (tyrosine aminotransferase 3)	–2.2	—	–4.33	—
At2g19190	FRK1 (flg22-induced receptor-like kinase 1)	–2.23	—	–3.46	—

Fold change in transcript abundance represented if significant regulation was found at $P<0.05$. NS, not significant.

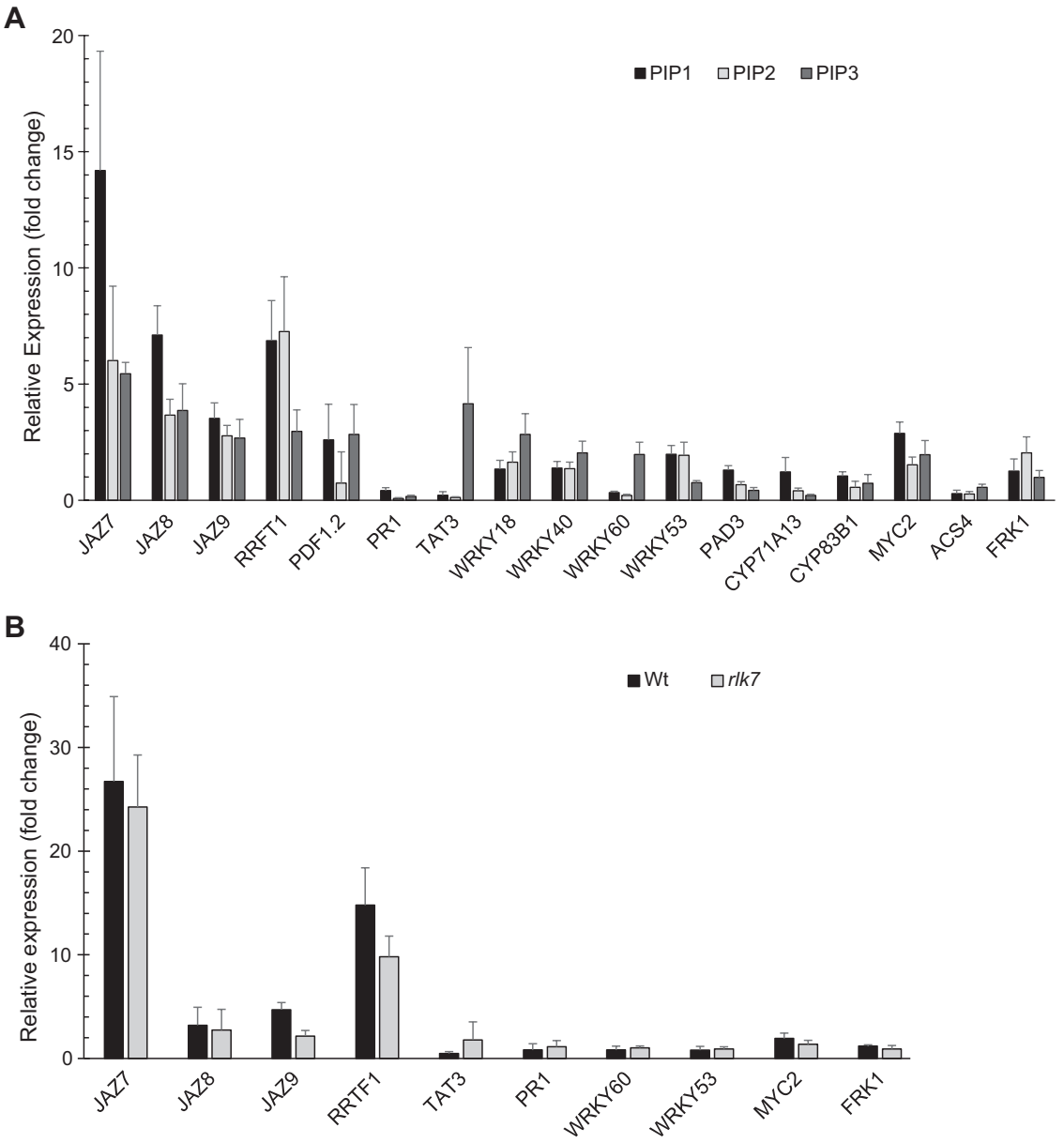

Fig. 2. (A) Exogenous application of PIP peptides changes the expression of immunity- related genes. Two-week-old seedlings were treated with 100 nM of the indicated peptides or water control for 3 h. Bars and error bars represent mean and standard deviation, respectively, calculated from three biological replicates. (B) RLK7 is less likely a major receptor for PIP3. Two-week-old WT and *rlk7* seedlings were treated by PIP3 synthetic peptide and control as described above for 3 h and gene expression for a selected set of genes in rosette leaves was analysed by qRT-PCR.

PIP3:OX plants. *fls2* was used as a negative control. Our assays showed a decrease in ROS production in *PIP3:OX* plants while a marginal increase was observed in *pip3* plants (Fig. 5B). Co-treatment of WT plants with flg22 and PIP3 peptides, but not flg22 and mock peptide, caused a marginal but not significant decrease in ROS production (Supplementary Fig. S3). Callose deposition in response to flg22 treatment was also quantified. Our data showed that *PIP3:OX* plants produce significantly ($P \leq 0.05$) less callose 24 h after flg22 treatment (Fig. 5C).

The enhanced susceptibility of plants overexpressing *PIP3* to flg22 prompted us to investigate whether PIP3 is involved in pathogen responses by infecting *pip3* and *PIP3:OX* seedlings with the hemibiotrophic bacterium *P. syringae* pv. *tomato* DC3000 (*Pst*). Plants overexpressing *PIP3* displayed enhanced susceptibility to *P. syringae* (Fig. 6A). In contrast, *pip3* plants showed a marginal but significant reduction in CFU at day 2 compared with WT. *Pseudomonas syringae* assays were also performed on 5-week-old soil-grown plants, with similar results (Supplementary Fig. S4).

We also investigated the response to the necrotrophic fungal *B. cinerea* isolate 2100 (Spanish type). Leaves of 5-week-old WT, *pip3*, and *PIP3:OX* lines were inoculated with a fungal spore suspension. WT Col-0 and *wrky33* mutant plants have been reported to be resistant and susceptible to this strain, respectively (Birkenbihl *et al.*, 2012). To evaluate the degree of susceptibility, we used *wrky33* as a susceptible control in our experiments. In WT and *pip3* plants, inoculation caused lesions at the site of infection 2 d after treatment, but development of necrotic lesions halted after day 3 (Fig. 6B). In contrast, the

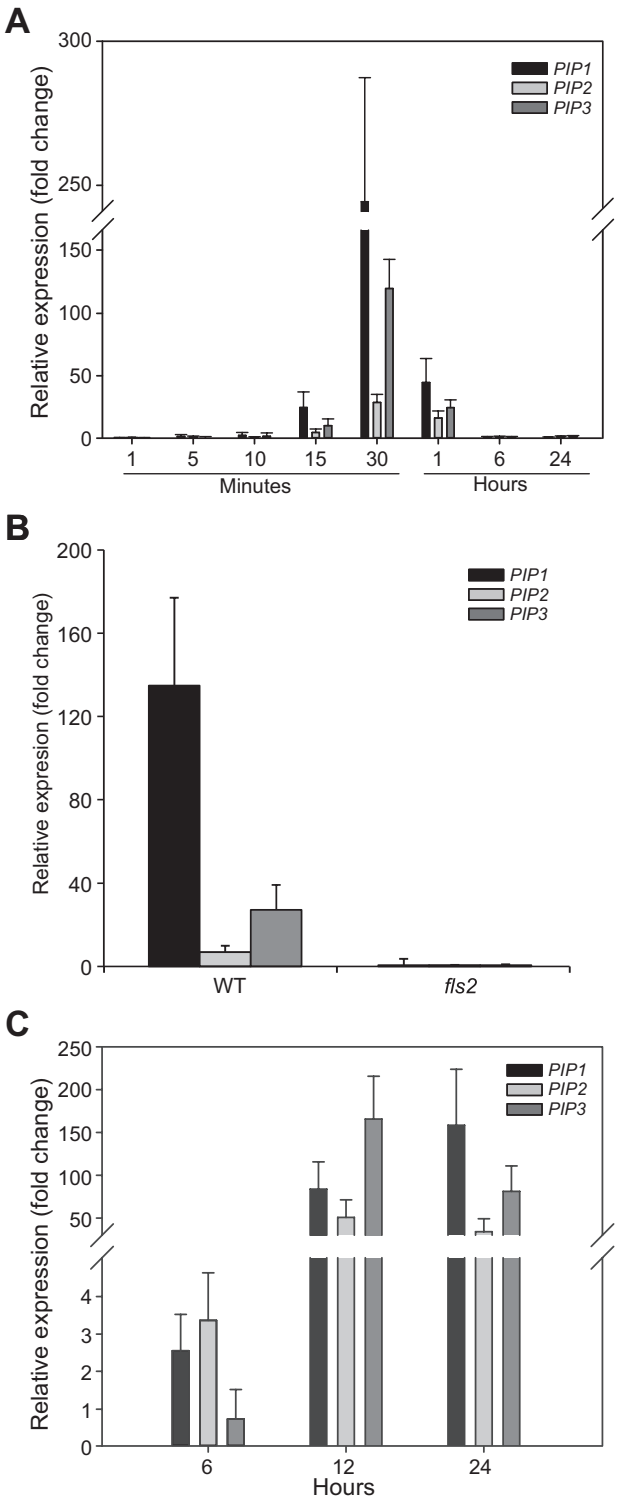

Fig. 3. flg22 treatment and *B. cinerea* infection induce *PIP* gene expression. (A) Time series analysis of *PIP1*, *PIP2*, and *PIP3* expression by qRT-PCR after flg22 treatment, compared with untreated tissue (n=4). (B) *PIP* expression in wild-type (WT) and *fls2* background 1 h after flg22 treatment (n=4). (C) Five-week-old plants grown under short day conditions were spray-inoculated with *B. cinerea* spores (5×10^5 ml^{-1}) or with Vogel buffer as control. Leaf tissue was harvested for RNA isolation and qRT-PCR analysis at indicated time points. Error bars represent the SD from three biological replicates.

symptoms developed much faster in *wrky33* plants and caused complete destruction of infected plants 5 d post-infection. The observed lesion sizes and symptoms in *PIP3:OX6* and

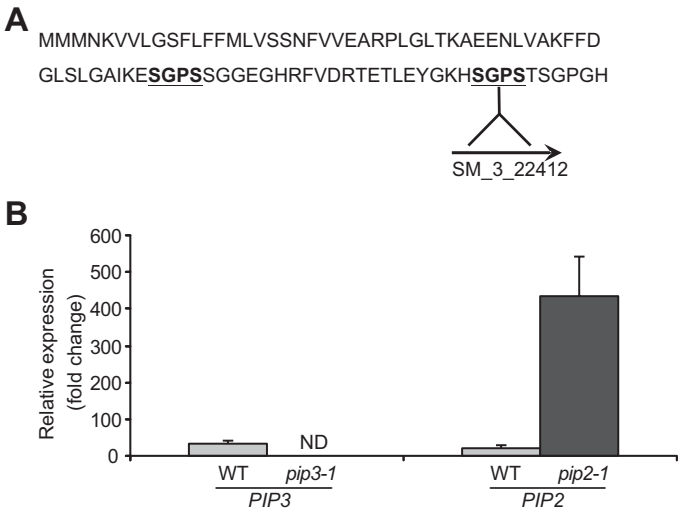

Fig. 4. Characterization and verification of *pip3*. (A) Amino acid sequence of PIP3. The two SGPS conserved motifs (underlined bold letters) and the transposon insertion are indicated. The arrow indicates transposon orientation. (B) Expression of *PIP3* and *PIP2* genes in WT and corresponding knockout lines 1 h after flg22 treatment. ND, not detectable. Error bars indicate the SD calculated from three biological replicates.

PIP3:OX7 lines were stronger compared with WT and *pip3* plants after day 2, and caused severe chlorosis in infected leaves after 5 d. However, in both evaluated *PIP3* overexpression lines, the symptom development rate and severity were much lower than in *wrky33* plants (Supplementary Fig. S5).

Successful colonization of host plants by *B. cinerea* and the degree of susceptibility was quantified as *in planta* fungal growth using qPCR analysis. Three days after inoculation, DNA from whole inoculated leaves were isolated and subjected to qPCR using *Bc*CutA and *At*SKII as pathogen and plant specific primers, respectively. The qPCR analysis showed a significantly higher ratio of *Bc*CutA/*At*SKII in *wrky33* in comparison with all other genotypes (Fig. 6C). However, *PIP3* overexpression lines also exhibited significantly elevated susceptibility compared with WT and *pip3* plants.

Together, the bioassay results showed that ectopic expression of *PIP3* negatively regulates the plant immune response when challenged by pathogens with different lifestyles.

Disease-related genes are differentially regulated in WT and PIP3 *overexpression plants*

To understand the altered disease phenotype in *PIP3* overexpression plants and to link it to known pathways, the temporal expression of disease-related genes was assessed. WT, *pip3*, and the *PIP3* overexpression line *PIP3:OX7* were inoculated with *B. cinerea* and leaf tissue was harvested for gene expression analysis 6, 12 and 24 hpi. The basal transcript level of the SA-inducible gene *PATHOGENESIS RELATED1* (*PR1*) was similar in all analysed genotypes; no strong induction was observed before 12 hpi (Fig. 7A). *PR1* transcript levels increased strongly in WT and *PIP3:OX7* plants after 12 hpi. At 24 hpi, *PR1* expression was significantly higher in *PIP3:OX7* plants compared with WT. Interestingly, no *PR1* induction was observed in *pip3* plants (Fig. 7A).

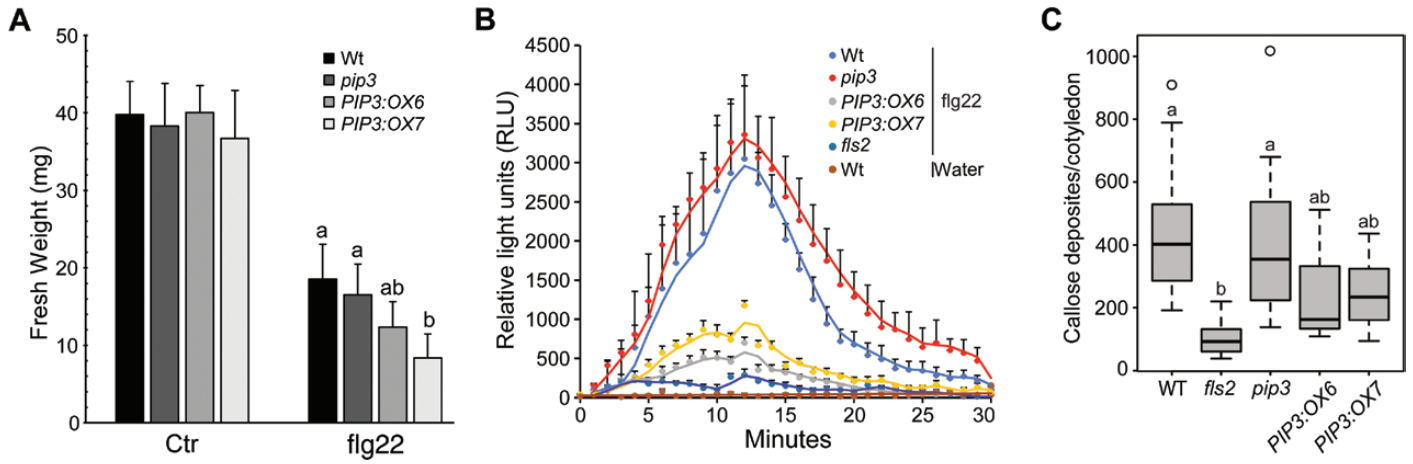

Fig. 5. *PIP3* overexpressing plants exhibit altered flg22-induced phenotypes. (A) Inhibition of seedling growth by flg22. Four-day-old seedlings grown on agar plate were transferred to liquid medium with 100 nM flg22 or without as control. Seedling fresh weight was measured 10 d after transfer. Error bars represent SD, n=24. Statistical analysis was performed using ANOVA and mean comparisons were done by Tukey–Kramer multiple test; letters indicate significant difference at (P<0.01). (B) Temporal production of ROS in response to flg22. Leaf disks from different genotypes of Arabidopsis plants were exposed to flg22. Water treatment of WT and flg22 treatment of *fls2* were used as negative controls. ROS production measured as luminescence was monitored over time as relative light units (RLU). The curves represent lines fitted to the data points of the ROS production over time. Error bars indicate SE, n=12. The whole experiment was repeated three times with similar results. (C) *PIP3* overexpression negatively affects callose deposition in response to flg22. Seven-day-old seedlings grown in six-well culture plates were exposed to fresh medium containing 1 μM of flg22 or control; 24 h after treatment, the seedlings were fixed and stained with aniline blue, and callose deposition at cotyledons was visualized and quantified. Statistical analysis (n=15) was performed using ANOVA and mean comparisons were done by Tukey–Kramer multiple test; letters indicate significant difference (P<0.05).

Based on the enhanced induction of *PR1* in *PIP3:OX* plants, we examined a set of genes involved in SA biosynthesis and signalling in *B. cinerea* challenged plants, including *ISOCHORISMATE SYNTHASE 1* (*ICS1*), the main gene in SA biosynthesis, *ENHANCED DISEASE SUSCEPTIBILITY 1* (*EDS1*), *NON-EXPRESSOR OF PR GENES 1* (*NPR1*), a master regulator of SA signalling, *EDS5*, and *PHYTOALEXIN DEFICIENT 4* (*PAD4*). Some common properties of the transcript responses were observed (Fig. 7B–F). For all genes, transcript induction at 24 hpi was strongest in *PIP3:OX7* plants (with the exception of *PAD4*).

We also evaluated the effect of altered *PIP3* expression on JA signalling upon *B. cinerea* infection. The JA-inducible gene *PLANT DEFENSIN1.2* (*PDF1.2*), as well as two key genes in JA biosynthesis (*AOC3* and *OPR3*) and three *JAZ* genes, were chosen for this analysis. The expression profile of *PDF1.2* showed the same pattern as for *PR1* up to 12 hpi, and the transcript levels increased by 24 hpi (Fig. 8A), with the expression levels of *PDF1.2* significantly higher in *PIP3:OX7* plants at 24 hpi compared with the other genotypes (P>0.05). *OPR3* was also upregulated in *PIP3:OX7* 24 hpi compared with WT and *pip3* (Fig. 8C). Interestingly, the expression levels of *AOC3* (Fig. 8B), *JAZ1* (Fig. 8D), *JAZ7* (Fig. 8E), and *JAZ8* (Fig. 8F) were significantly induced in *PIP3:OX7* plants at both 12 hpi and 24 hpi, but unchanged or moderately induced in WT as well as in *pip3*.

PIPs *are regulated by WRKY transcription factors*

Sequence analysis of *PIP1*, *PIP2*, and *PIP3* revealed that the promoter regions of these genes are enriched in W-boxes, which are target sites for binding of WRKY TFs. *In silico* data suggest that the expression of *PIPs* is affected in *wrky33* and *wrky18/40* plants (Birkenbihl *et al.*, 2017). To further investigate this, we analysed the expression levels of *PIP1-3* in *wrky18*, *40* and *33* knockout mutants. *PIP1-3* expression was not affected in *wrky18* nor *wrky40* single knockout plants (Fig. 9). In contrast, *PIP1* and *PIP3* expression increased significantly in the *wrky18/40* double mutant. Similar analysis revealed that *PIP2* and *PIP3* expression was significantly induced in *wrky33* background. These results indicate that WRKY18, WRKY40, and WRKY33 function cooperatively as repressors of *PIP1-3*. This observation is consistent with previous studies, which have shown that WRKY18 and WRKY40 are able to bind DNA as heterodimers (Xu *et al.*, 2006; Chen *et al.*, 2010; Pandey *et al.*, 2010). To further support these observations, genome-wide ChiP-seq data revealed that the promoter regions of *PIP1*, *PIP2*, and *PIP3* are occupied by WRKY18, WRKY40, and WRKY33 2 h after flg22 treatment (Supplementary Fig. S6), while WRKY33 actively binds to the promoter regions of *PIP1* and *PIP3* 14 h after infection by *B. cinerea* (Supplementary Fig. S7).

Discussion

Plant peptides are derived from different genomic sources and are engaged in a plethora of functions in plant growth, development, and stress responses (Tavormina *et al.*, 2015). However, only a fraction of them, including IDA, have been assigned to a biological function (Butenko *et al.*, 2003). We have previously studied the phylogeny and expression of the *IDA/IDL* and *PIP/PIPL* gene families showing, that several *PIP* genes are highly inducible by different biotic and abiotic stresses (Vie *et al.*, 2015). Hou *et al.* (2014) reported that PIP1 amplifies plant immune responses against biotrophic and necrotrophic pathogens through RLK7. The present study aimed to further

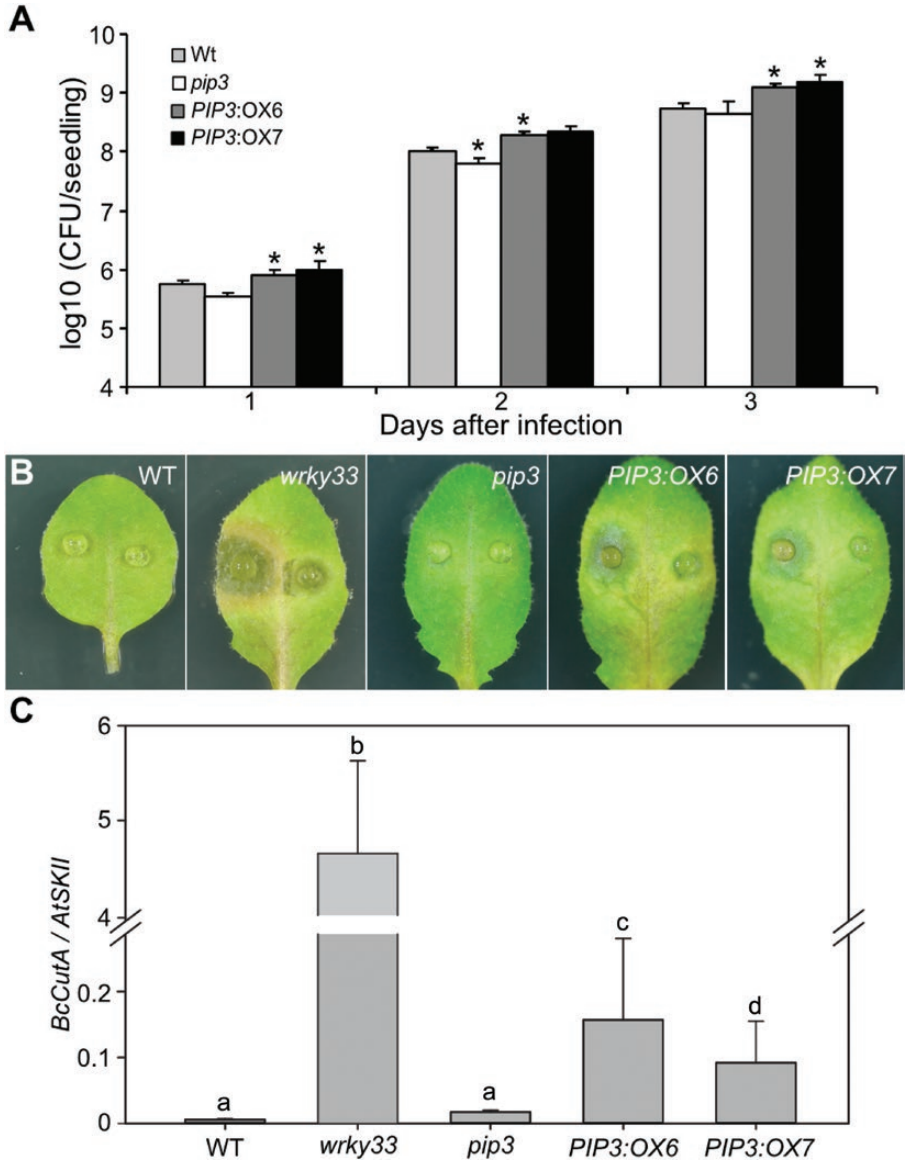

Fig. 6. *PIP3* overexpressing plants show increased susceptibility to *Pseudomonas syringae* and *Botrytis cinerea.* (A) Seven-day-old seedlings were co-cultivated with *P. syringae* pv. *tomato* DC3000. Bacterial growth rate was measured as colony forming units (CFU) at 1, 2, and 3 d after inoculation (DAI). Bars and error bars represent means and SD, respectively, calculated from four biological replicates. Each replicate consists of three seedlings (Supplementary Dataset S2). The whole experiment was repeated at least three times with similar results. Statistical analysis was performed using two-tailed *t*-test; *significant difference ($P<0.05$) compared with WT at the corresponding day. (B) Disease symptoms of 5-week-old detached leaves infected with spores of *B. cinerea* isolate 2100 3 d post-infection. (C) Quantification of *B. cinerea* growth 3 d after inoculation with fungal spores. The relative abundance of *B. cinerea* and Arabidopsis DNA was determined by qPCR using pathogen-specific (*Bc*CutA) and plant-specific (*At*SKII) primers. Bars and error bars represent mean and SD, respectively ($n=3$). Statistical analysis was performed using ANOVA and mean comparisons were done by Tukey–Kramer multiple test; letters indicate significant difference ($P<0.05$).

elucidate the role of the related PIP3 peptide in regulation of the plant immune response. The PIP3 prepropeptide contains two conserved SGPS motifs (Fig. 4). These two motifs might result in two distinguished mature peptides with the ability to activate independent pathways under different conditions or to be incorporated in a single pathway by binding to different receptor partners. Such a phenomenon has been reported for CLAVATA3/ESR-RELATED 18 (CLE18). The CLE18 peptide was first reported as an inhibitor of tracheary element differentiation and root growth (Ito *et al.*, 2006), whereas another active peptide form of CLE18 has been described to promote root growth (Meng *et al.*, 2012). Another study showed that synthetic peptides for the C-terminal SGPS motifs of PIP2 and PIP3 were found to inhibit lateral root development, while no effect was observed for the N-terminal SGPS motif peptides (Ghorbani *et al.*, 2015). Thus, the C-terminal SGPS motif might be the major contributor to the biological activity; alternatively, the N-terminal SGPS motif might be important in other processes or tissues. Structural flexibility of prepropeptides to produce different final active forms provides an extra layer of complexity in studies of signal transduction pathways initiated by peptide hormones.

Plant immunity consists of a complex network of different hormonal and protein signalling cascades with synergistic or

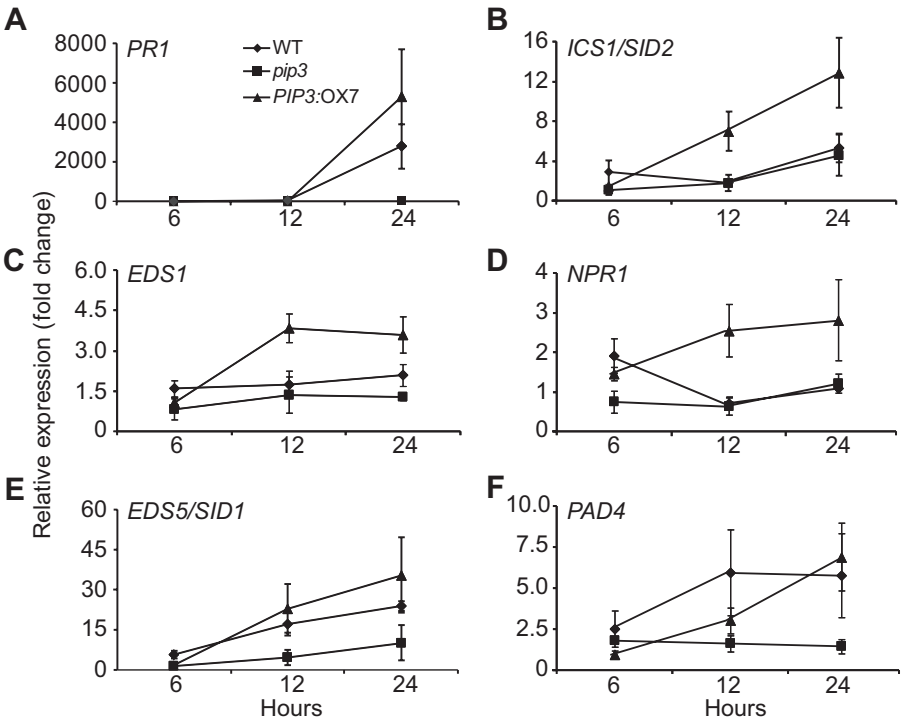

Fig. 7. Expression patterns of salicylic acid biosynthesis- and signalling-related genes upon *B. cinerea* infection. Transcript levels were determined by qRT-PCR at indicated time points relative to the mock treatment at 6 h post-infection. Error bars represent SD from three biological replicates.

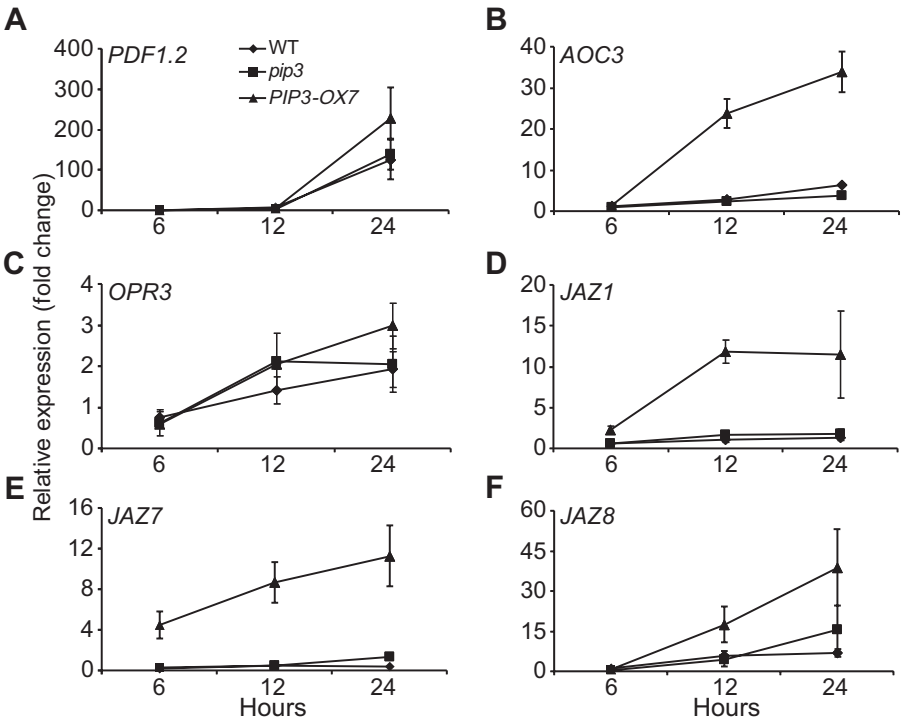

Fig. 8. Expression patterns of jasmonic acid biosynthesis- and signalling-related genes upon *B. cinerea* infection. Transcript levels were determined by qRT-PCR at indicated time points relative to the mock treatment at 6 h post-infection. Error bars represent SD from three biological replicates.

antagonistic cross-talk depending on the nature of the invader and their lifestyle (Jonak *et al.*, 2002; Spoel *et al.*, 2003; Pieterse *et al.*, 2012; Berens *et al.*, 2017). Activation of the plant immune system is a highly energy-demanding process and can affect plant growth adversely. Due to the limited available resource pool, a tight regulatory mechanism should control growth–defence trade-offs in plants to avoid unnecessary activation of the immune system (Huot *et al.*, 2014). Our results show that ectopic application of the conserved C-terminal domains of PIP1, PIP2, and PIP3 peptides leads to differential regulation

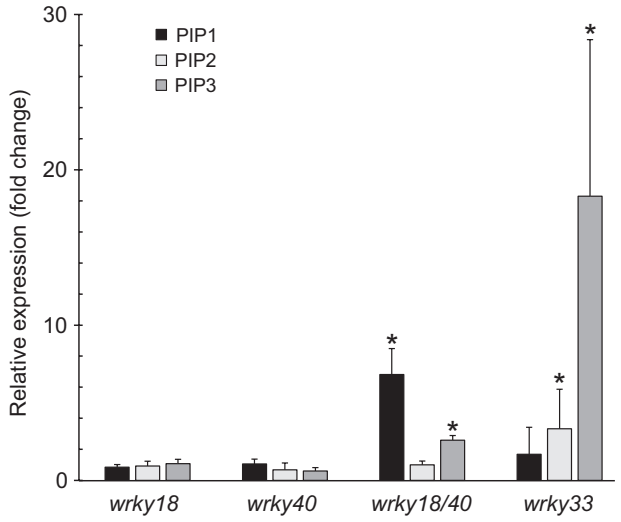

Fig. 9. *PIP1* and *PIP3* expression is repressed by the WRKY18/40 and WRKY33 complex. Wild-type and knockout plants were grown on ½MS agar plates for 2 weeks. Rosette leaf tissue was harvested for RNA isolation and qRT-PCR analysis. Bars and error bars represent mean and SD, respectively (n=3). Expression level was assessed relative to wild-type plants grown under similar conditions. Statistical differences (Student's t-test: *P<0.05) between wild-type and mutants are indicated.

of many genes involved in defence-related phytohormone (SA, JA and ET) biosynthesis and signalling pathways, as well as redox homeostasis (Table 1; Figs 1, 2A).

flg22 and *B. cinerea* treatment of WT plants strongly induced the expression of *PIP1*, *PIP2*, and *PIP3* (Fig. 3). In addition, seedling growth inhibitory assays in the presence of flg22 revealed that plants overexpressing *PIP3* are hypersensitive to flg22 (Fig. 5A), suggestive of a role for PIP3 in the regulation of plant response to pathogens. Recognition of PAMPs or pathogen-derived effectors by their cognitive receptors initiates a biphasic oxidative burst composed of fast and slow steps that are correlated to PTI and ETI, respectively (Grant and Loake, 2000). During the early stage of PAMP perception, a rapid oxidative burst is triggered by plasma membrane localized Respiratory Burst Oxidase Homologs (RBOHs) that leads to accumulation of H_2O_2 in the apoplastic space. Elevated ROS levels in the apoplast are toxic to pathogens, and mediate fast, long-distance, cell-to-cell propagation of a ROS signalling wave (Miller *et al.*, 2009). Vie *et al.* (2017) showed that IDL6 and IDL7 act as negative modulators of stress-induced ROS signalling in Arabidopsis. Our data showed a significant decrease of ROS production in response to flg22 in *PIP3:OX* plants (Fig. 5B). Whether this effect is caused by activation of ROS scavenging mechanisms or repression of ROS-producing RBOHs remains to be shown. However, co-treatment of WT plants with flg22 and PIP3 did not change the ROS accumulation significantly (Supplementary Fig. S3).

PIP1 is perceived by RLK7, which activates the MAP kinases MPK3 and MPK6 through a MAP kinase cascade (Hou *et al.*, 2014). RBOH activity is regulated at the post-translational level by phosphorylation (Baxter *et al.*, 2014, Kadota *et al.*, 2014). The MAP kinase kinase kinase MKKK7 was found to interact with FLS2 and attenuate both ROS bursts and MPK6 activation downstream of FLS2 (Mithoe *et al.*, 2016). In view of our results, MKKK7 would be an attractive downstream candidate for PIP3 and its receptor. Another interesting target that can correlate ROS accumulation levels to plant response to pathogens is Redox Responsive Transcription Factor 1 (RRTF1). The expression of *RRTF1* is significantly induced by exogenous application of PIP1–3 peptides (Table 1; Fig. 2). It has been shown that *RRTF1* inactivation restricts and *RRTF1* overexpression induces ROS accumulation in response to stresses. Furthermore, plants overexpressing *RRTF1* were highly susceptible to infection by the necrotrophic fungus *Alternaria brassicae* (Matsuo *et al.*, 2015). Regulation of *RRTF1* expression by *A. brassicae* infection, high light, and H_2O_2 was also shown to require WRKY18/40/60. In line with this hypothesis, our promoter analysis showed that WRKY18/40 heterodimer and WRKY33 act as negative regulators of *PIP1*, *PIP2*, and *PIP3* expression (Fig. 9). In addition, WRKY factors can bind to the promoter of *PIPs* during biotic stresses (Supplementary Figs S6, S7). Altogether, our data suggest that PIP3 might be involved in attenuation of ROS production and subsequent systemic signalling, possibly as part of a negative feedback controlling system to avoid runaway responses.

The altered susceptible phenotype of *PIP3:OX* plants when challenged by pathogens with different lifestyles (Figs 5B, 6) supports the hypothesis that PIP3 is involved in the modulation of plant immunity through regulation of SA and JA signalling pathways (Figs 7, 8). Plants have evolved different mechanisms to fight off pathogens based on their invasion strategies. In order to discriminate biotrophs from necrotrophs, plants use phytohormones to activate and regulate appropriate responses. SA is a major regulator when plants are challenged by biotrophs (Tsuda *et al.*, 2008; Vlot *et al.*, 2009), while responses to necrotrophs and herbivorous insects mainly are mediated by JA and ET (Farmer *et al.*, 2003; Kachroo and Kachroo, 2009; Berens *et al.*, 2017). SA and JA signalling pathways are generally antagonistic to each other. When plants encounter multiple pathogens with different lifestyles simultaneously, internal cross-talk between SA and JA signalling pathways optimizes the proper response. It has been shown that under this situation, synergistic and compensatory relationships between signalling pathways drive the final response by the host plant (Tsuda *et al.*, 2009). Simultaneous activation of JA and SA biosynthesis results in suppression of JA signalling by the SA pathway. SA triggers cell death, which acts in favour of necrotrophs (Glazebrook, 2005; Spoel and Dong, 2008; Caarls *et al.*, 2015). The observed susceptible phenotype of *PIP3:OX* plants infected by *B. cinerea* can be explained in line with this concept. However, the temporal regulation of SA and JA biosynthesis and signalling genes by overexpression of *PIP3* is not able to explain the observed susceptible phenotype of *PIP3:OX* plants challenged by the biotroph pathogen *Pst* DC 3000. A recent study has shown that when Arabidopsis plants are challenged by *Pst* DC 3000 avirulent strain carrying avrRpt2, both SA and JA pathways are induced simultaneously but in different zones relative to the infection site (Betsuyaku *et al.*, 2018). This study showed that 13 h after infection, the SA active zone surrounds the infection site where the hypersensitive reaction takes place, while JA signalling is exclusively activated in cell layers outside of the SA active zone. According to our

gene expression analysis after PIP3 and flg22 treatments (Figs 2, 3), we hypothesize that upon perception of pathogens, PIP3 might play a positive role in spatiotemporal regulation of SA and JA signalling pathways to mount a proper defence response based on pathogen invasion strategy. Our data indicate that this spatiotemporal regulation is compromised in *PIP3:OX* plants. The actual mechanistic role of PIP3 in this process remains to be tested experimentally. Hou *et al.* (2014) reported that PIP1 signals through RLK7, causing an amplification of the immune response against pathogens. There are differences in the experimental set-ups that may explain the contradictory observed responses to the synthetic peptides. Hou *et al.* used shorter PIP1 and PIP2 synthetic peptide (13 and 15 aa, respectively) that were hydroxylated at the last proline (P-OH) within the SGPS motif. It has been shown that post-translational modifications can change peptide activities. Furthermore, Hou *et al.* applied synthetic peptides at micromolar concentrations in all of their assays, whereas we used unmodified longer synthetic peptides at 100 nM concentration. Studies on synthetic CLE40 peptide and its effect on root growth have revealed that depending on the nature of modifications and concentrations of applied peptide in the growth medium, CLE40 can repress or induce root growth of soybean plants (Corcilius *et al.*, 2017). However, our data suggest that RLK7 is less likely to be a major receptor for PIP3, as *rlk7* plants responded similarly to WT plants when treated with PIP3 peptide (Fig. 2B).

In conclusion, our results show that signalling triggered by the small peptides PIP1, PIP2, and PIP3 can reprogram the expression of genes encoding proteins involved in regulation of plant immunity. Furthermore, ectopic expression or exogenous application of PIP3 peptide changes the expression of genes involved in immune response towards attenuation of immunity. Based on our data, we propose a model in which expression of *PIP3* is cooperatively repressed by WRKY18/40 and WRKY33 under normal conditions (Fig. 10A). Perception of PAMPs by corresponding PRRs induces the expression of *PreproPIP3*. Preproproteins are then transported to the apoplast and proteolytically processed to produce mature peptides. Perception of mature PIP3 peptide by its corresponding cell surface receptors initiates new signalling pathways that result in the suppression of PAMP-induced genes. Induction of *WRKY18*, *WRKY40*, and *WRKY33* expression by PAMPs as well as PIP3 results in a negative feedback loop that restricts *PIP3* expression temporally and/or spatially. When *PIP3* overexpression plants are challenged by *B. cinerea*, both SA and JA biosynthesis and signalling pathways are transcriptionally induced (Fig. 10B). Simultaneous activation of SA and JA pathways upon pathogen attack prioritize SA over JA. One outcome of this interaction is hypersensitive reaction and cell death, facilitating growth and colonization of the host plant by necrotrophic pathogens (Fig. 10). An alternative explanation is the spatiotemporal regulation of SA and JA activities by PIP3 as discussed above. The potential role of these peptides in growth and development should be unveiled by analysis of *PIP1* and *PIP2* knockout/silencing plants, alone or in combination with *pip3*. In addition, identification of the postulated PIP3 receptor(s) will shed light on the downstream events and components involved in signalling, as well as their possible cross-talks with phytohormones.

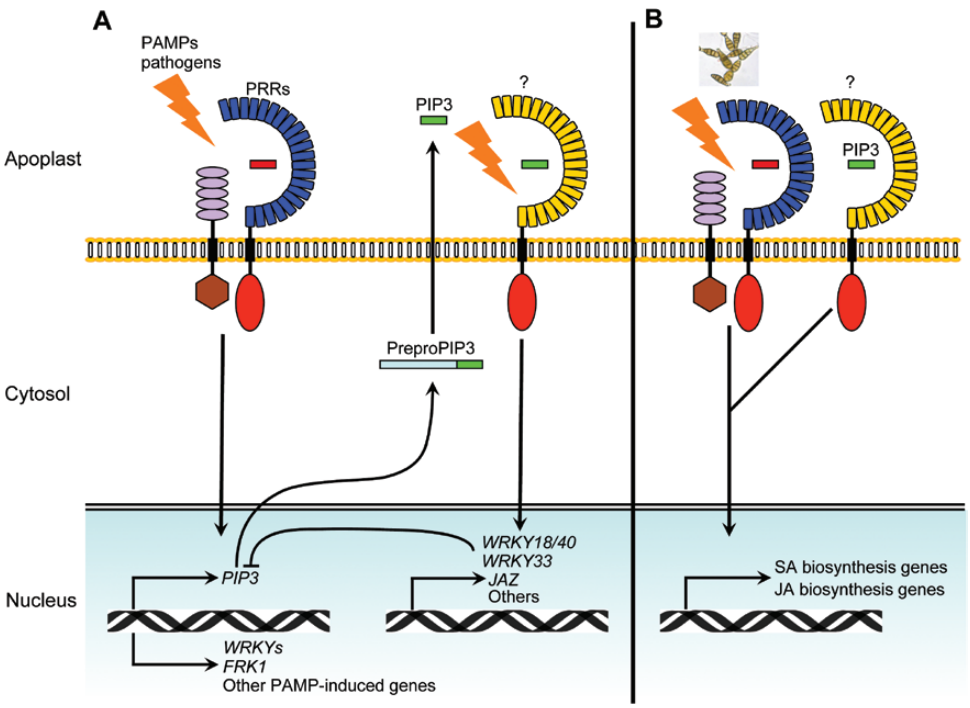

Fig. 10. Proposed model for PIP3-modulated signalling of plant immunity. (A) *PIP3* transcript level is induced by perception of PAMPs and/or pathogens through PRRs. Mature PIP3 is sensed by its corresponding receptors located at the plasma membrane. Exogenous application of PIP3 peptide leads to induction of *JAZ* genes as well as *WRKY18* and *WRKY40*. WRKY18, WRKY40, and WRKY33 may act in a negative feedback loop to terminate *PIP3* expression. (B) *PIP3* overexpression plants challenged by *B. cinerea* simultaneously activate the expression of JA and SA biosynthesis and signalling genes. The outcome of the interaction between SA and JA is hypersensitive reaction, cell death, and susceptibility to *B. cinerea*.

Supplementary data

Supplementary data are available at *JXB* online.

Dataset S1. PIP1–3 and PEP1–3 co-expression tables.

Dataset S2. Differentially regulated genes upon PIP1 and PIP2 peptide treatments.

Fig. S1. Co-expression analysis of *PIP1*, *PIP2*, and *PIP3*.

Fig. S2. Expression and phenotype analysis of *PIP3* overexpression lines.

Fig. S3. Temporal production of ROS in response to flg22 and PIP3 peptides.

Fig. S4. Susceptibility of 5-week-old *pip3* and *PIP3:OX* plants to *P. syringae*.

Fig. S5. Disease symptoms of 5-week-old plants 5 d after inoculation with 5×10^5 ml^{-1} of *B. cinerea* spores.

Fig. S6. Binding of WRKY18, WRKY40, and WRKY33 to *PIP1*, *PIP2*, and *PIP3* promoter regions in response to flg22 treatment.

Fig. S7. Binding of WRKY33 to *PIP1* and *PIP3* promoter regions in response to *B. cinerea* infection.

Table S1. List of primers used in this study.

Table S2. Expression pattern of *PIP1*, *PIP2* and *PIP3* in response to the different elicitors in wild-type (Col-0) and *fls2* backgrounds obtained from public databases.

Acknowledgements

We appreciate the excellent technical assistance of Torfinn Sparstad. The authors also acknowledge Prof. Shigeyuki Betsuyaku (University of Tsukuba, Ibaraki, Japan) for critical reading of the manuscript and his comments. JN was funded by FUGE (Norwegian Functional Genomics) program. AKV was funded by the Research Council of Norway by grant 230757. This work was partly supported by the Deutsche Forschungsgemeinschaft (DFG) grant SFB670 (IS).

References

Abràmoff MD, Magalhães PJ, Ram SJ. 2004. Image processing with ImageJ. Biophotonics International **11**, 36–43.

Baxter A, Mittler R, Suzuki N. 2014. ROS as key players in plant stress signalling. Journal of Experimental Botany **65**, 1229–1240.

Berens ML, Berry HM, Mine A, Argueso CT, Tsuda K. 2017. Evolution of hormone signaling networks in plant defense. Annual Review of Phytopathology **55**, 401–425.

Betsuyaku S, Katou S, Takebayashi Y, Sakakibara H, Nomura N, Fukuda H. 2018. Salicylic acid and jasmonic acid pathways are activated in spatially different domains around the infection site during effector-triggered immunity in *Arabidopsis thaliana*. Plant & Cell Physiology **59**, 8–16.

Birkenbihl RP, Diezel C, Somssich IE. 2012. Arabidopsis WRKY33 is a key transcriptional regulator of hormonal and metabolic responses toward *Botrytis cinerea* infection. Plant Physiology **159**, 266–285.

Birkenbihl RP, Kracher B, Roccaro M, Somssich IE. 2017. Induced genome-wide binding of three Arabidopsis WRKY transcription factors during early MAMP-triggered immunity. The Plant Cell **29**, 20–38.

Bisceglia NG, Gravino M, Savatin DG. 2015. Luminol-based assay for detection of immunity elicitor-induced hydrogen peroxide production in *Arabidopsis thaliana* leaves. Bio-Protocol **5**, e1685.

Boller T, Flury P. 2012. Peptides as danger signals: MAMPs and DAMPs. In: Irving HR, Gehring C, eds. Plant signalling peptides. Berlin, Heidelberg: Springer, 163–181.

Butenko MA, Patterson SE, Grini PE, Stenvik GE, Amundsen SS, Mandal A, Aalen RB. 2003. Inflorescence deficient in abscission controls floral organ abscission in *Arabidopsis* and identifies a novel family of putative ligands in plants. The Plant Cell **15**, 2296–2307.

Caarls L, Pieterse CM, Van Wees SC. 2015. How salicylic acid takes transcriptional control over jasmonic acid signaling. Frontiers in Plant Science **6**, 170.

Chen H, Lai Z, Shi J, Xiao Y, Chen Z, Xu X. 2010. Roles of arabidopsis WRKY18, WRKY40 and WRKY60 transcription factors in plant responses to abscisic acid and abiotic stress. BMC Plant Biology **10**, 281.

Chisholm ST, Coaker G, Day B, Staskawicz BJ. 2006. Host-microbe interactions: shaping the evolution of the plant immune response. Cell **124**, 803–814.

Clough SJ, Bent AF. 1998. Floral dip: a simplified method for *Agrobacterium*-mediated transformation of *Arabidopsis thaliana*. The Plant Journal **16**, 735–743.

Corcilius L, Hastwell AH, Zhang M, Williams J, Mackay JP, Gresshoff PM, Ferguson BJ, Payne RJ. 2017. Arabinosylation modulates the growth-regulating activity of the peptide hormone CLE40a from soybean. Cell Chemical Biology **24**, 1347–1355.e7.

Denoux C, Galletti R, Mammarella N, Gopalan S, Werck D, De Lorenzo G, Ferrari S, Ausubel FM, Dewdney J. 2008. Activation of defense response pathways by OGs and Flg22 elicitors in *Arabidopsis* seedlings. Molecular Plant **1**, 423–445.

Earley KW, Haag JR, Pontes O, Opper K, Juehne T, Song K, Pikaard CS. 2006. Gateway-compatible vectors for plant functional genomics and proteomics. The Plant Journal **45**, 616–629.

Farmer EE, Alméras E, Krishnamurthy V. 2003. Jasmonates and related oxylipins in plant responses to pathogenesis and herbivory. Current Opinion in Plant Biology **6**, 372–378.

Felix G, Duran JD, Volko S, Boller T. 1999. Plants have a sensitive perception system for the most conserved domain of bacterial flagellin. The Plant Journal **18**, 265–276.

Gachon C, Saindrenan P. 2004. Real-time PCR monitoring of fungal development in *Arabidopsis thaliana* infected by *Alternaria brassicicola* and *Botrytis cinerea*. Plant Physiology and Biochemistry **42**, 367–371.

Ghorbani S, Lin YC, Parizot B, Fernandez A, Njo MF, Van de Peer Y, Beeckman T, Hilson P. 2015. Expanding the repertoire of secretory peptides controlling root development with comparative genome analysis and functional assays. Journal of Experimental Botany **66**, 5257–5269.

Gilroy S, Suzuki N, Miller G, Choi WG, Toyota M, Devireddy AR, Mittler R. 2014. A tidal wave of signals: calcium and ROS at the forefront of rapid systemic signaling. Trends in Plant Science **19**, 623–630.

Glazebrook J. 2005. Contrasting mechanisms of defense against biotrophic and necrotrophic pathogens. Annual Review of Phytopathology **43**, 205–227.

Gómez-Gómez L, Boller T. 2000. FLS2: an LRR receptor-like kinase involved in the perception of the bacterial elicitor flagellin in *Arabidopsis*. Molecular Cell **5**, 1003–1011.

Grant JJ, Loake GJ. 2000. Role of reactive oxygen intermediates and cognate redox signaling in disease resistance. Plant Physiology **124**, 21–29.

Hanai H, Matsuno T, Yamamoto M, Matsubayashi Y, Kobayashi T, Kamada H, Sakagami Y. 2000. A secreted peptide growth factor, phytosulfokine, acting as a stimulatory factor of carrot somatic embryo formation. Plant & Cell Physiology **41**, 27–32.

Hou S, Wang X, Chen D, Yang X, Wang M, Turrà D, Di Pietro A, Zhang W. 2014. The secreted peptide PIP1 amplifies immunity through receptor-like kinase 7. PLoS Pathogens **10**, e1004331.

Huffaker A, Pearce G, Ryan CA. 2006. An endogenous peptide signal in *Arabidopsis* activates components of the innate immune response. Proceedings of the National Academy of Sciences, USA **103**, 10098–10103.

Huot B, Yao J, Montgomery BL, He SY. 2014. Growth-defense tradeoffs in plants: a balancing act to optimize fitness. Molecular Plant **7**, 1267–1287.

Igarashi D, Tsuda K, Katagiri F. 2012. The peptide growth factor, phytosulfokine, attenuates pattern-triggered immunity. The Plant Journal **71**, 194–204.

Ito Y, Nakanomyo I, Motose H, Iwamoto K, Sawa S, Dohmae N, Fukuda H. 2006. Dodeca-CLE peptides as suppressors of plant stem cell differentiation. Science **313**, 842–845.

Jonak C, Okrész L, Bögre L, Hirt H. 2002. Complexity, cross talk and integration of plant MAP kinase signalling. Current Opinion in Plant Biology **5**, 415–424.

Jones JD, Dangl JL. 2006. The plant immune system. Nature **444**, 323–329.

Kachroo A, Kachroo P. 2009. Fatty acid-derived signals in plant defense. Annual Review of Phytopathology **47**, 153–176.

Kadota Y, Sklenar J, Derbyshire P, *et al*. 2014. Direct regulation of the NADPH oxidase RBOHD by the PRR-associated kinase BIK1 during plant immunity. Molecular Cell **54**, 43–55.

Karpinski S, Reynolds H, Karpinska B, Wingsle G, Creissen G, Mullineaux P. 1999. Systemic signaling and acclimation in response to excess excitation energy in *Arabidopsis*. Science **284**, 654–657.

Krol E, Mentzel T, Chinchilla D, *et al*. 2010. Perception of the *Arabidopsis* danger signal peptide 1 involves the pattern recognition receptor AtPEPR1 and its close homologue AtPEPR2. The Journal of Biological Chemistry **285**, 13471–13479.

Kwon SJ, Jin HC, Lee S, Nam MH, Chung JH, Kwon SI, Ryu CM, Park OK. 2009. GDSL lipase-like 1 regulates systemic resistance associated with ethylene signaling in Arabidopsis. The Plant Journal **58**, 235–245.

Lee H, Chah OK, Sheen J. 2011. Stem-cell-triggered immunity through CLV3p-FLS2 signalling. Nature **473**, 376–379.

Ligterink W, Kroj T, zur Nieden U, Hirt H, Scheel D. 1997. Receptor-mediated activation of a MAP kinase in pathogen defense of plants. Science **276**, 2054–2057.

Liu S, Kracher B, Ziegler J, Birkenbihl RP, Somssich IE. 2015. Negative regulation of ABA signaling by WRKY33 is critical for *Arabidopsis* immunity towards *Botrytis cinerea* 2100. eLife **4**, e07295.

Luna E, Pastor V, Robert J, Flors V, Mauch-Mani B, Ton J. 2011. Callose deposition: a multifaceted plant defense response. Molecular Plant-Microbe Interactions **24**, 183–193.

Lyons R, Iwase A, Gänsewig T, *et al*. 2013. The RNA-binding protein FPA regulates flg22-triggered defense responses and transcription factor activity by alternative polyadenylation. Scientific Reports **3**, 2866.

Matsubayashi Y, Sakagami Y. 1996. Phytosulfokine, sulfated peptides that induce the proliferation of single mesophyll cells of *Asparagus officinalis* L. Proceedings of the National Academy of Sciences, USA **93**, 7623–7627.

Matsuo M, Johnson JM, Hieno A, *et al*. 2015. High REDOX RESPONSIVE TRANSCRIPTION FACTOR1 levels result in accumulation of reactive oxygen species in *Arabidopsis thaliana* shoots and roots. Molecular Plant **8**, 1253–1273.

Melotto M, Underwood W, Koczan J, Nomura K, He SY. 2006. Plant stomata function in innate immunity against bacterial invasion. Cell **126**, 969–980.

Meng L, Buchanan BB, Feldman LJ, Luan S. 2012. CLE-like (CLEL) peptides control the pattern of root growth and lateral root development in *Arabidopsis*. Proceedings of the National Academy of Sciences, USA **109**, 1760–1765.

Miller G, Schlauch K, Tam R, Cortes D, Torres MA, Shulaev V, Dangl JL, Mittler R. 2009. The plant NADPH oxidase RBOHD mediates rapid systemic signaling in response to diverse stimuli. Science Signaling **2**, ra45.

Mithoe SC, Ludwig C, Pel MJ, *et al*. 2016. Attenuation of pattern recognition receptor signaling is mediated by a MAP kinase kinase kinase. EMBO Reports **17**, 441–454.

Mittler R, Vanderauwera S, Gollery M, Van Breusegem F. 2004. Reactive oxygen gene network of plants. Trends in Plant Science **9**, 490–498.

Mosher S, Seybold H, Rodriguez P, *et al*. 2013. The tyrosine-sulfated peptide receptors PSKR1 and PSY1R modify the immunity of Arabidopsis to biotrophic and necrotrophic pathogens in an antagonistic manner. The Plant Journal **73**, 469–482.

Mostafavi S, Ray D, Warde-Farley D, Grouios C, Morris Q. 2008. GeneMANIA: a real-time multiple association network integration algorithm for predicting gene function. Genome Biology **9**(Suppl 1), S4.

Nakano T, Suzuki K, Ohtsuki N, Tsujimoto Y, Fujimura T, Shinshi H. 2006. Identification of genes of the plant-specific transcription-factor families cooperatively regulated by ethylene and jasmonate in *Arabidopsis thaliana*. Journal of Plant Research **119**, 407–413.

Nürnberger T, Brunner F, Kemmerling B, Piater L. 2004. Innate immunity in plants and animals: striking similarities and obvious differences. Immunological Reviews **198**, 249–266.

Obayashi T, Aoki Y, Tadaka S, Kagaya Y, Kinoshita K. 2018. ATTED-II in 2018: a plant coexpression database based on investigation of the statistical property of the mutual rank index. Plant & Cell Physiology **59**, e3.

Pandey SP, Roccaro M, Schön M, Logemann E, Somssich IE. 2010. Transcriptional reprogramming regulated by WRKY18 and WRKY40 facilitates powdery mildew infection of Arabidopsis. The Plant Journal **64**, 912–923.

Pieterse CM, Van der Does D, Zamioudis C, Leon-Reyes A, Van Wees SC. 2012. Hormonal modulation of plant immunity. Annual Review of Cell and Developmental Biology **28**, 489–521.

Qiu JL, Fiil BK, Petersen K, *et al*. 2008. Arabidopsis MAP kinase 4 regulates gene expression through transcription factor release in the nucleus. The EMBO Journal **27**, 2214–2221.

Sessions A, Burke E, Presting G, *et al*. 2002. A high-throughput *Arabidopsis* reverse genetics system. The Plant Cell **14**, 2985–2994.

Sewelam N, Kazan K, Schenk PM. 2016. Global plant stress signaling: reactive oxygen species at the cross-road. Frontiers in Plant Science **7**, 187.

Spoel SH, Dong X. 2008. Making sense of hormone crosstalk during plant immune responses. Cell Host & Microbe **3**, 348–351.

Spoel SH, Koornneef A, Claessens SM, *et al*. 2003. NPR1 modulates cross-talk between salicylate- and jasmonate-dependent defense pathways through a novel function in the cytosol. The Plant Cell **15**, 760–770.

Tavormina P, De Coninck B, Nikonorova N, De Smet I, Cammue BP. 2015. The plant peptidome: an expanding repertoire of structural features and biological functions. The Plant Cell **27**, 2095–2118.

Tissier AF, Marillonnet S, Klimyuk V, Patel K, Torres MA, Murphy G, Jones JD. 1999. Multiple independent defective suppressor-mutator transposon insertions in *Arabidopsis*: a tool for functional genomics. The Plant Cell **11**, 1841–1852.

Tsuda K, Sato M, Glazebrook J, Cohen JD, Katagiri F. 2008. Interplay between MAMP-triggered and SA-mediated defense responses. The Plant Journal **53**, 763–775.

Tsuda K, Sato M, Stoddard T, Glazebrook J, Katagiri F. 2009. Network properties of robust immunity in plants. PLoS Genetics **5**, e1000772.

Van der Does D, Leon-Reyes A, Koornneef A, *et al*. 2013. Salicylic acid suppresses jasmonic acid signaling downstream of SCFCOI1-JAZ by targeting GCC promoter motifs via transcription factor ORA59. The Plant Cell **25**, 744–761.

Vie AK, Najafi J, Liu B, Winge P, Butenko MA, Hornslien KS, Kumpf R, Aalen RB, Bones AM, Brembu T. 2015. The *IDA/IDA-LIKE* and *PIP/PIP-LIKE* gene families in *Arabidopsis*: phylogenetic relationship, expression patterns, and transcriptional effect of the PIPL3 peptide. Journal of Experimental Botany **66**, 5351–5365.

Vie AK, Najafi J, Winge P, Cattan E, Wrzaczek M, Kangasjärvi J, Miller G, Brembu T, Bones AM. 2017. The IDA-LIKE peptides IDL6 and IDL7 are negative modulators of stress responses in *Arabidopsis thaliana*. Journal of Experimental Botany **68**, 3557–3571.

Vlot AC, Dempsey DA, Klessig DF. 2009. Salicylic acid, a multifaceted hormone to combat disease. Annual Review of Phytopathology **47**, 177–206.

Xia XJ, Zhou YH, Shi K, Zhou J, Foyer CH, Yu JQ. 2015. Interplay between reactive oxygen species and hormones in the control of plant development and stress tolerance. Journal of Experimental Botany **66**, 2839–2856.

Xu X, Chen C, Fan B, Chen Z. 2006. Physical and functional interactions between pathogen-induced *Arabidopsis* WRKY18, WRKY40, and WRKY60 transcription factors. The Plant Cell **18**, 1310–1326.

Yamaguchi Y, Huffaker A, Bryan AC, Tax FE, Ryan CA. 2010. PEPR2 is a second receptor for the Pep1 and Pep2 peptides and contributes to defense responses in *Arabidopsis*. The Plant Cell **22**, 508–522.